Nuclear Engineering and Technology 50 (2018) 280–291

Contents lists available at ScienceDirect

Nuclear Engineering and Technology

journal homepage: www.elsevier.com/locate/net

Original Article

Uncertainty and sensitivity analysis in reactivity-initiated accident fuel modeling: synthesis of organisation for economic co-operation and development (OECD)/nuclear energy agency (NEA) benchmark on reactivity-initiated accident codes phase-II

Olivier Marchand [a, *], Jinzhao Zhang [b], Marco Cherubini [c]

[a] Institut de Radioprotection et de Sûreté Nucléaire (IRSN), PSN-RES, SEMIA, Cadarache, St Paul-Lez-Durance, 13115, France
[b] Tractebel (ENGIE), Avenue Ariane 7, 1200 Brussels, Belgium
[c] Nuclear and Industrial Engineering (NINE), Borgo Giannotti 19, 55100 Lucca, Italy

ARTICLE INFO

Article history:
Received 18 October 2017
Received in revised form
6 December 2017
Accepted 18 December 2017
Available online 17 January 2018

Keywords:
RIA
Codes Benchmarking
Fuel Modelling
OECD

ABSTRACT

In the framework of OECD/NEA Working Group on Fuel Safety, a RIA fuel-rod-code Benchmark Phase I was organized in 2010–2013. It consisted of four experiments on highly irradiated fuel rodlets tested under different experimental conditions. This benchmark revealed the need to better understand the basic models incorporated in each code for realistic simulation of the complicated integral RIA tests with high burnup fuel rods. A second phase of the benchmark (Phase II) was thus launched early in 2014, which has been organized in two complementary activities: (1) comparison of the results of different simulations on simplified cases in order to provide additional bases for understanding the differences in modelling of the concerned phenomena; (2) assessment of the uncertainty of the results. The present paper provides a summary and conclusions of the second activity of the Benchmark Phase II, which is based on the input uncertainty propagation methodology. The main conclusion is that uncertainties cannot fully explain the difference between the code predictions. Finally, based on the RIA benchmark Phase-I and Phase-II conclusions, some recommendations are made.
© 2018 Korean Nuclear Society, Published by Elsevier Korea LLC. This is an open access article under the CC BY-NC-ND license (http://creativecommons.org/licenses/by-nc-nd/4.0/).

1. Introduction

Reactivity-initiated accidents (RIA) are nuclear reactor accidents that involve unwanted increase in fission rate and reactor power. A rapid power excursion leads to an adiabatic heating of the fuel pellets and may lead to failure of the fuel rod. Thereon, a large part of the fuel pellet inventory could be dispersed into the coolant. Fuel-coolant interaction could cause pressure pulses or rapid steam generation, which could damage not only fuel assemblies or other core components but also the reactor pressure vessel. The fuel rod behavior during RIA has to be analyzed to verify its compliance with safety criteria [1].

RIA fuel rod codes have been developed for a significant period of time and validated against their own available database. However, the high complexity of the scenarios dealt with has resulted in a number of different models and assumptions adopted by code developers; additionally, databases used to develop and validate codes have been different depending on the availability of the results of some experimental programs. This diversity makes it difficult to find the source of estimation discrepancies, when these occur.

A technical workshop on “Nuclear Fuel Behavior During Reactivity-Initiated Accidents” was organized by the nuclear energy agency (NEA) of the organisation for economic co-operation and development (OECD) in September 2009 [2]. A major highlight from the session devoted to RIA safety criteria was that RIA fuel rod codes are now widely used, within the industry as well as the technical safety organizations, in the process of setting up and assessing revised safety criteria for RIA design basis accidents. This turns mastering the use of these codes into an outstanding milestone, particularly in safety analyses. To achieve that, a thorough understanding of code predictability is mandatory.

At the conclusion of the workshop, it was recommended that a benchmark (RIA benchmark Phase I) between these codes be organized to give a sound basis for their comparison and assessment. To maximize the benefits from this RIA benchmark Phase I exercise, it was decided to use a consistent set of four experiments using fuel

* *Corresponding author.*
E-mail address: olivier.marchand@irsn.fr (O. Marchand).

https://doi.org/10.1016/j.net.2017.12.007
1738-5733/© 2018 Korean Nuclear Society, Published by Elsevier Korea LLC. This is an open access article under the CC BY-NC-ND license (http://creativecommons.org/licenses/by-nc-nd/4.0/).

rodlets refabricated from similar high-burnup full-length rods under different experimental conditions. A detailed and complete RIA benchmark Phase I specification was prepared to ensure, as much as possible, the comparability of the calculation results submitted [3].

The main conclusions of the RIA benchmark Phase I are the following [4]:

- With respect to the thermal behavior, the differences in the evaluation of fuel temperatures remained consistent with each other, although these differences were significant in some cases. The situation was very different for the cladding temperatures that exhibited considerable scatter, in particular for cases when water boiling occurred.
- With respect to mechanical behavior, the parameter of largest interest was the cladding hoop strain, because failure during RIA transient results from the formation of longitudinal cracks. When compared to the results of an experiment that involved only pellet clad mechanical interaction, the predictions from the different participants appeared acceptable even though there was a factor of 2 between the highest and the lowest calculations. This conclusion was not so favorable for cases in which water boiling had been predicted to appear: a factor of 10 for the hoop strain between the calculations was exhibited. Other mechanical results compared during the RIA benchmark Phase I were fuel stack and cladding elongations. The scatter remained limited for the fuel stack elongation, but the cladding elongation was found to be much more difficult to evaluate.
- The fission-gas release evaluations were also compared. The ratio of the maximum to the minimum values appeared to be roughly two, which is considered to be relatively moderate given the complexity of fission gas release processes.
- Failure predictions, which may be considered as the ultimate goal of fuel code dedicated to the behavior in RIA conditions, were compared: it appears that the failure/no failure predictions are fairly consistent between the different codes and the experimental results. However, when assessing the code qualification, one should rather look at predictions in terms of enthalpy at failure because it is a parameter that may vary significantly between different predictions (and is also of interest in practical reactor applications). In the frame of this RIA benchmark Phase I, the failure prediction levels among the different codes were within a ±50% range.

As a conclusion of the RIA benchmark Phase I, it was recommended to launch a second phase exercise with the following specific guidelines:

- The emphasis should be put on deeper understanding of the differences in modeling of the different codes; in particular, looking for simpler cases than those used in the first exercise was expected to reveal the main reasons for the observed large scatter in some conditions such as coolant boiling.
- Owing to the large scatter between the calculations that was shown in the RIA benchmark Phase I, it appears that an assessment of the uncertainty of the results should be performed for the different codes. This should be based on a well-established and shared methodology. This also entailed performing a sensitivity study of results to input parameters to assess the impact of initial state of the rod on the final outcome of the power pulse.

The second phase of the RIA fuel rod code benchmark (RIA benchmark Phase II) was launched early in 2014. This RIA benchmark Phase II has been organized as two complementary activities [5,6]:

- The first activity is to compare the results of different simulations on simplified cases to provide additional bases for understanding the differences in modeling of the concerned phenomena.
- The second activity is focused on the assessment of the uncertainty of the results. In particular, the impact of the initial states and key models on the results of the transient are investigated.

The present article provides the specification (§2), the participants and their adopted codes (§3), a detailed comparison of the results (§4), and conclusions and recommendations from the second activity (§5).

2. Benchmark specification

The objective of this second activity of the RIA benchmark Phase II [7] was to assess the uncertainty of the results. In particular, the impact of the initial states and key models on the results of the transient behavior of fuel rods was investigated. All uncertainties were considered as either statistical or random ones. The identification and treatment of epistemic uncertainties, if any, was beyond the scope of the project. In addition, a sensitivity study was performed to identify or confirm the most influential input uncertainties.

2.1. Description of the reference case

Considering the feedback from Phase I of the RIA benchmark, the uncertainty analysis was initially intended to be performed on the foreseen CABRI international program test, CIP3-1, on an irradiated ZIRLO-cladded UO_2 fuel rodlet in pressurized water reactor (PWR) representative conditions. This case was also considered in Phase I of the benchmark and resulted in the largest differences in the predictions from the different codes [4]. However, in the first activity of Phase II, it appeared that, despite simplifications in the defined cases, a significant spread of results was still present. The original thought of using the CIP3-1 case (interesting due to its high burnup) seemed too ambitious for the reference case due to the complex initial rod state evaluation, the large effort required from participants and the risk of nonconclusive outcomes.

Therefore, it was agreed that the numerical reference case should be “Case 5” for the first activity (see Refs. [5] and [6]). To limit the differences linked to the initial state of the fuel, the case is limited to a fresh 17 × 17 PWR-type fuel rodlet, as described in Fig. 1, with standard UO_2 fuel pellet without dish and chamfer and Zircloy-4 cladding. It is also assumed that there is no initial gap between the fuel and the clad; these are considered perfectly bonded from the mechanical point of view. The upper plenum is pressurized with helium at a typical pressure of a PWR rod (2 MPa at 20°C).

The thermal-hydraulic conditions during the transient are representative of water coolant in nominal PWR hot zero power conditions (coolant inlet conditions: $P_{cool} = 15.5$ MPa, $T_{cool} = 280$°C and $V_{cool} = 4$ m/s). These conditions are established by letting the coolant pressure and temperature increase linearly from ambient conditions over 50 seconds, after which a 50 seconds pretransient hold time is postulated to establish steady-state conditions. The reference pulse starts from zero power at t-100 seconds. It is considered to have a triangular shape, with 30 ms of full width at half maximum (FWHM). A high value for the rod maximal power in the fuel is considered to lead to a specific injected energy of 127 cal/g. This value should provoke departure from nucleate boiling.

All parameters of rod design and boundary conditions are specified in Table 1.

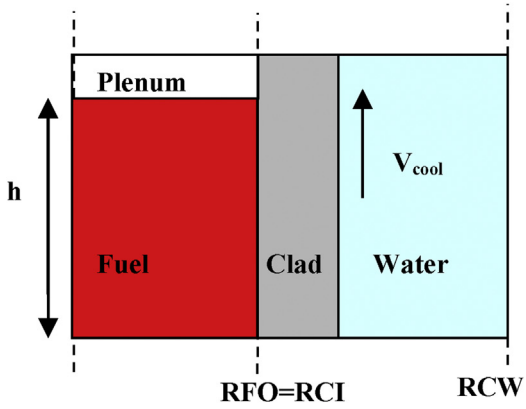

Fuel outer radius (RFO) = 4.13 mm
Clad inner radius (RCI) = 4.13 mm
Clad thickness = 570 μm
Water canal radius (RCW) = 7.5 mm
Upper plenum volume =2 cm^3
Fuel height (h) = 10 cm
Coolant velocity (V_{cool}) = 4.0 m/s

Fig. 1. Benchmark rod design.

Table 1
List of input uncertainty parameters for statistical uncertainty analysis.

Input uncertainty parameter	Distribution				
	Mean	Standard deviation	Type	Lower bound	Upper bound
1. Fuel rod manufacturing tolerances					
Cladding outside diameter (mm)	9.40	0.01	Normal	9.38	9.42
Cladding inside diameter (mm)	8.26	0.01	Normal	8.24	8.28
Fuel theoretical density (kg/m^3 at 20°C)	10970	50	Normal	10870	11070
Fuel porosity %	4	0.5	Normal	3	5
Cladding roughness (μm)	0.1	1	Normal	10^{-6}	2
Fuel roughness (μm)	0.1	1	Normal	10^{-6}	2
Filling gas pressure (MPa)	2.0	0.05	Normal	1.9	2.1
2. Thermal hydraulic boundary conditions					
Coolant pressure (MPa)	15.500	0.075	Normal	15.350	15.650
Coolant inlet temperature (°C)	280	1.5	Normal	277	283
Coolant velocity (m/s)	4.00	0.04	Normal	3.92	4.08
3. Core power boundary conditions					
Injected energy in the rod (Joule)	30000	1500	Normal	27000	33000
Full width at half maximum (ms)	30	5	Normal	20	40
4. Physical properties/key models					
Fuel thermal conductivity model (multiple coefficient)	1.00	5%	Normal	0.90	1.10
Clad thermal conductivity model (multiple coefficient)	1.00	5%	Normal	0.90	1.10
Fuel thermal expansion model (multiple coefficient)	1.00	5%	Normal	0.90	1.10
Clad thermal expansion model (multiple coefficient)	1.00	5%	Normal	0.90	1.10
Clad yield stress (multiple coefficient)	1.00	5%	Normal	0.90	1.10
Fuel enthalpy/heat capacity (multiple coefficient)	1.00	1.5%	Normal	0.97	1.03
Clad-to-coolant heat transfer (multiple coefficient—Same coefficient applied for all flow regimes)	1.00	12.5%	Normal	0.75	1.25

2.2. Methodology

Among all the available uncertainty analysis methods, the probabilistic input uncertainty propagation method is, so-far, the most widely used in nuclear safety analysis [8]. In this method, the fuel codes are treated as “black boxes”, and the input uncertainties are propagated to the simulation model output uncertainties via the code calculations, with sampled data from known or assumed distributions as key input parameters [9]. The input parameters of interest may also include uncertain material properties, model parameters, etc. The method consists of the following steps:

1) Specification of the problem: all relevant code outputs and corresponding uncertain parameters for the codes, plant modeling schemes, and plant operating conditions are identified.
2) Uncertainty modeling: the uncertainty of each uncertain parameter is quantified by a probability density function (PDF) based on engineering judgment and experience feedback from code applications to separate and integral effect tests and to full plant simulation. If dependencies between uncertain parameters are known and judged to be potentially important, they can be quantified by correlation coefficients.
3) Uncertainty propagation through the computer code: the propagation is represented by Monte Carlo simulations [10]. In Monte Carlo simulations, the computer code is run repeatedly, each time using different values for each of the uncertain parameters. These values are drawn from the probability distributions and dependencies chosen in the previous step. In this way, one value for each uncertain parameter is sampled simultaneously in each repetition of the simulation. The results of a Monte Carlo simulation lead to a sample of the same size for each output quantity.
4) Statistical analysis of the results: the output sample is used to obtain typical statistics of the code response such as mean or variance and to determine the cumulative distribution function. The cumulative distribution function enables the derivation of the percentiles of the distribution.

The probabilistic input uncertainty propagation method was selected because of its simplicity, robustness, and transparency.

Based on the OECD best estimate methods, uncertainty and sensitivity evaluation program (BEMUSE) recommendations [11], the sample size is set to 200 (i.e., 200 code runs must be performed). The sample is constructed according to the selected PDFs coming from the uncertainty modeling step and assuming independence between input parameters following a simple random sampling. Normal distribution was assigned for all the considered input parameters, only for simplicity. A parametric study using uniform distribution for a specific code was performed, and the results are quite comparable. For real applications, one must justify or quantify the distribution for each input parameter.

We focus on the estimation of a lower, respectively upper, uncertainty bound (LUB, respectively UUB) (LUB, of the 5%, respectively 95%, percentiles at confidence level higher than 95%.

Besides uncertainty analysis, a complementary study was performed to obtain qualitative insights into the most influential input parameters. This work was done based on a global sensitivity analysis using the 200 code runs previously obtained. The sensitivity measures are based on Spearman rank correlation coefficient; an arbitrary significance threshold of 0.25 is chosen for influential input parameters.

2.3. Uncertainty parameters and output specification

The uncertainties from Phase I and activity 1 of Phase II of the RIA benchmark, as well as the OECD benchmark for uncertainty analysis en modelling (UAM) [12], were identified and classified into four categories: Uncertainties in the fuel rod design, bounded by allowable manufacturing tolerances, thermal-hydraulic boundary conditions, core power boundary conditions, and physical properties/key models.

Table 1 provides the specified input parameters as well as information related to their uncertainty. For each input parameter, the information includes a mean value, a standard deviation, and a type of distribution. To avoid unphysical numerical values, a range of variation (lower and upper bounds) was also provided. The sampling was performed between the upper and lower bounds, i.e., the PDFs were truncated. To simplify the current benchmark application, a normal distribution was assigned to all the considered input parameters. Their standard deviation was taken as the half of the maximum of the absolute value of the difference between their nominal value and their upper or lower bound for all input parameters, except for the cladding roughness and fuel roughness, for which a standard deviation of one was assumed, but the upper or lower bounds were set.

For simplicity, the uncertainty of the pulse width was considered independently from that of the injected energy. The uncertainties of certain relevant thermal properties (calculated by built-in empirical models as a function of temperature) were also considered.

The effect of the uncertainty modeling (i.e., the choice of a normal distribution and the correlation between input parameters) was not studied in this benchmark. Although this effect could have some impact on the derived uncertainty bands, the conclusions of this exercise are expected to be similar for other distributions. It should be recalled that, as this study is limited to fresh fuel, uncertainty parameters for irradiated fuel (such as fission gases distribution, cladding corrosion, gap conductance …) are not considered here. Finally, although the dependency between the pulse width and the injected energy is well known, it was not considered.

As a result of the uncertainty analysis, each participant gave lower and upper uncertainty bounds associated with all the time trends of the output parameters listed in Table 2. In addition, the results of the calculation with the nominal values of the input parameters, also called the reference calculation, were provided. The reference and the lower and upper uncertainty bound values were also provided for the following scalar outputs: maximum value for each parameter in Table 2, time to maximum value for each parameter and for the boiling duration, difference between time of critical heat flux achievement, and time of reaching the rewetting heat flux.

Table 2
List of time-dependent output parameters.

Parameter	Unit	Description
DHR	cal/g	Variation of radial average enthalpy with respect to initial conditions of the transient in the rodlet as a function of time (at z = h/2) [please note that: DHR (t = 0) = 0]
TFC	°C	Temperature of fuel centerline as a function of time (at z = h/2)
TFO	°C	Temperature of fuel outer surface as a function of time (at z = h/2)
TCO	°C	Temperature of clad outer surface as a function of time (at z = h/2)
ECTH	%	Clad total (thermal + elastic + plastic) hoop strain at the outer part of the clad as a function of time (at z = h/2)
ECT	mm	Clad total axial elongation as a function of time
EFT1	mm	Fuel column total axial elongation as a function of time
SCH	MPa	Clad hoop stress at outer part of the clad as a function of time (at z = h/2)
RFO	mm	Fuel outer radius as a function of time (at z = h/2)

Thanks to those data provided by each participant, it has been possible to compute the main quantities of interest for all outputs parameters:

- The uncertainty band for one code and one output parameter, which is the interval [LUB, UUB],
- The uncertainty band width for one code and one output parameter, which is the difference between UUB and LUB,
- The global uncertainty width for output parameter, which is the difference between the maximum of all UUB and the minimum of all LUB,
- The reference calculation dispersion for one output parameter, which is the difference between the maximum and the minimum value of the parameter for all reference calculations.

For scalar output, the relative global uncertainty interval was also defined as the interval [Minimum (LUB), Maximum (UUB)] divided by the average of all reference calculations.

To evaluate the agreement or disagreement between the results, a conflict indicator has been built (see [7] for more details). On one hand, if the indicator is near one, this means that there is an important disagreement between all the results (i.e., empty intersection between all uncertainty intervals). On the other hand, if the indicator is near zero it means that we have good agreement between all simulations (i.e., large overlapping between all uncertainty intervals).

Regarding sensitivity analysis, the Spearman rank correlation coefficient associated with each uncertain input for each output at the different defined times as well as for their maximal values was also provided by all participants. The most influential input parameters have been identified for each participant, based on their calculated correlation coefficients and using a fixed significance

threshold of 0.25. To draw conclusions for practical issues, the results have been summarized with respect to groups of outputs corresponding to a type of behavior (fuel thermal, clad thermal, clad mechanical, and fuel mechanical behavior). More precisely, several outputs have been aggregated together following the rule that if an input parameter is influential for an output associated with a given behavior, it is considered as influential for the whole group.

3. Participants and codes used

Participation in the benchmark has been very important and 14 organizations provided solutions. The participants, which represented 12 countries, are listed below:

- Tractebel (ENGIE) from Belgium,
- ÚJV Řež (UJV) from the Czech Republic,
- Institut de Radioprotection et de Sûreté Nucléaire (IRSN) and Commissariat à l'énergie atomique et aux énergies alternatives (CEA) from France,
- Gesellschaft für Anlagen-und Reaktorsicherheit (GRS) GmbH from Germany,
- Centre of Energy Research, Hungarian Academy of Sciences (MTA-EK) from Hungary,
- Nuclear and Industrial Engineering (NINE) from Italy,
- Japan Atomic Energy Agency (JAEA) from Japan,
- Korea Institute of Nuclear Safety (KINS) from Korea,
- Centro de Investigaciones Energéticas, Medioambientales y Tecnológicas (CIEMAT) and Consejo de Seguridad Nuclear (CSN) from Spain,
- Strålsäkerhetsmyndigheten (Swedish Radiation Safety Authority—SSM) represented by Quantum Technologies from Sweden,
- Nuclear Regulatory Commission (USNRC) and Idaho National Laboratory (INL) in collaboration with Utah State University (USU) from the Unites States,
- VTT Technical Research Centre of Finland (VTT) from Finland.

In terms of computer fuel rod codes used, the spectrum was also large as solutions were provided with ALCYONE, BISON, FRAPTRAN, RANNS, SCANAIR, TESPA-ROD, and TRANSURANUS. Table 3 summarizes the contributions provided by the participants, the codes used for transient simulation as well as for sensitivity and uncertainty analyses, and the labels used to identified each contribution in figures.

4. Comparison of main results

4.1. Uncertainty analysis: time trend outputs

During the power deposit, there is a very good agreement between all the participants for fuel thermal behavior. As an example, concerning the reference calculations, the discrepancy for the maximal fuel centerline temperature (TFC) is lower than 40°C (see Fig. 2). The TFC uncertainty assessment with respect to time is also quite consistent between all the participants. During the power deposit, the uncertainty band width can be very high, around 800°C (see Fig. 3). This result is linked to the fact that the uncertainty of the pulse width is very large (±10 ms). Thus, even with the same final injected energy, the injected energy 40 ms after the beginning of the transient can vary by a factor of two in the two extreme cases of pulse half width (20 ms and 40 ms), which can lead to large thermal differences during the transient. Just after the power deposit, the TFC uncertainty is significantly lower, 200–300°C, which is 10–15% of the TFC reference value (~1850°C).

The same "pulse width uncertainty effect" can be seen in other parameters during the transient: very large during the power deposit, much less after the pulse [see Figs. 4 and 5 for the clad hoop strain—(ECTH)]. One can notice that the uncertainty is rather significant for the mechanical parameter during the pulse (see Fig. 4).

After the power deposit, all participants calculate boiling at the clad-to-coolant interface. The thermomechanical behavior of the rod will mainly depend on the clad-to-coolant heat transfer coefficient and on the quenching time. The uncertainty evolutions of the clad thermal and mechanical results are represented in Figs. 6 and 7. The uncertainty is still large after the power deposit for all the participants, both for thermal [clad outer temperature (TCO)] and mechanical output [clad hoop stress (SCH)]. The discrepancies between participants are significant, mainly due to different modeling of the heat transfer during the boiling phase and to significant difference in quenching time. SCH uncertainty is also affected by the mechanical approach (i.e., different yield stress laws).

Figs. 8 and 9 show the reference calculation dispersion and the global uncertainty width for fuel enthalpy variation (DHR) and TCO. The global uncertainty width is close to the reference calculation dispersion. The code effect is very significant here. As illustrated for TCO in Fig. 9, for several outputs, the reference calculation dispersion is larger than the typical uncertainty resulting from input parameter variations calculated by each participant individually.

Table 3
Benchmark collected contributions (organizations and code combinations used).

Organization		Codes used	
Name	Label on figures	Transient calculation	Sensitivity and uncertainty analyses
SSM	SSM-A	SCANAIR V_7_5	SUNSET
	SSM-B	SCANAIR V_7_5 + TH-2P	SUNSET
VTT	VTT	SCANAIR V_7_5	SUSA
IRSN	IRSN	SCANAIR V_7_6	SUNSET
CIEMAT	CIEMAT	SCANAIR V_7_5	Internal tool
USNRC	USNRC	FRAPTRAN V2.0	DAKOTA
UJV	UJV	FRAPTRAN V_1_5	internal tool
KINS	KINS	FRAPTRAN V2.0	SUNSET
TRACTEBEL	TRACTEBEL	FRAPTRAN V2.0-Beta	DAKOTA
MTA-EK	MTA-EK	FRAPTRAN 1.4.-TRABCO_unc	Internal tool
NINE	NINE	TRANSURANUS	Internal tool
JAEA	JAEA	RANNS	DAKOTA
GRS	GRS	TESPA-ROD	SUSA
CEA	CEA	ALCYONE 1.4	URANIE
INL	INL	BISON	DAKOTA

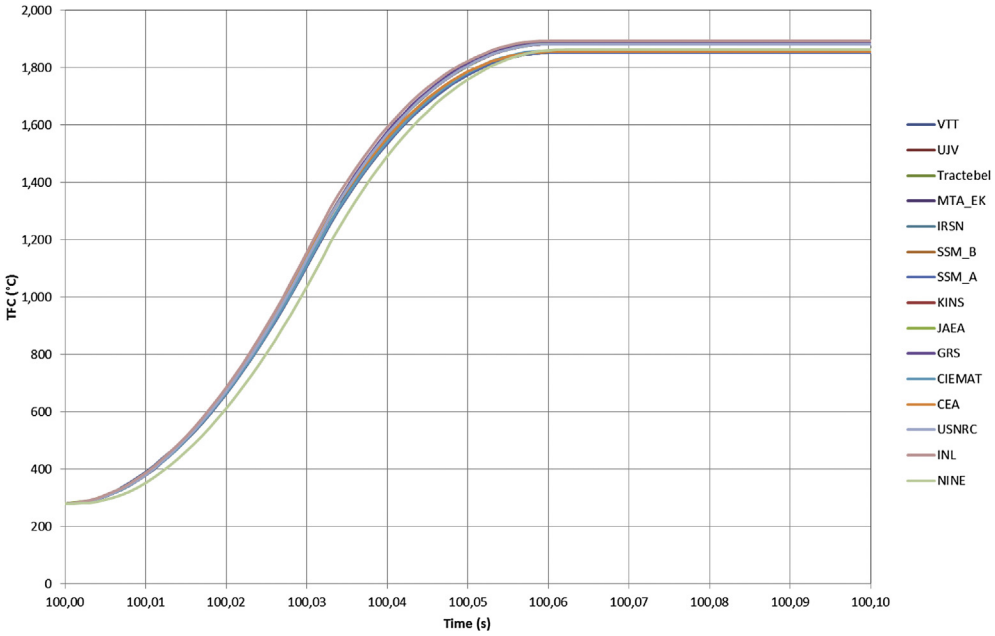

Fig. 2. TFC reference calculations.

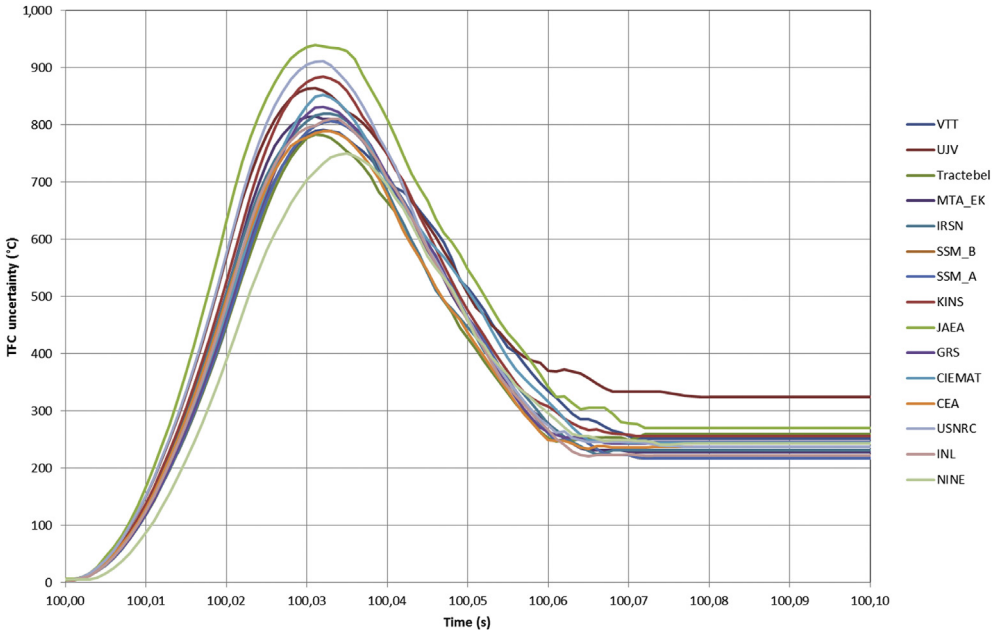

Fig. 3. TFC uncertainty band widths.

4.2. Uncertainty analysis: scalar outputs

Fig. 10 displays the relative global uncertainty associated with each scalar output parameter related to maximum values and boiling duration, taking into account the contributions of all participants. The results show that the global uncertainty interval width depends on the type of parameter observed. More precisely, the narrowest relative uncertainty intervals are obtained for fuel thermal behavior outputs (DHR, TFC, and TFO with a factor less than 1.5 between upper and lower bounds). The uncertainty interval width increases slightly for fuel mechanical outputs and clad elongation (RFO, EFT1, and ECT with a factor between 2 and 2.5) and more significantly for other clad mechanical outputs and clad temperature (ECTH, SCH, and TCO). Concerning this last group, SCH exhibits a larger uncertainty (a factor ~5) than ECTH (a factor ~2.5). Finally, the largest uncertainty interval is observed for the boiling duration (a factor ~30).

To evaluate the agreement or disagreement between participants' contributions, the conflict indicator for each output was used. It appears that the results are highly conflicting, except for fuel thermal behavior (see Fig. 11). However, by construction, this indicator is equal to one as soon as two participants fully disagree (i.e., empty intersection between their uncertainty intervals). By investigating the reasons for this lack of coherence, three levels of coherence were identified:

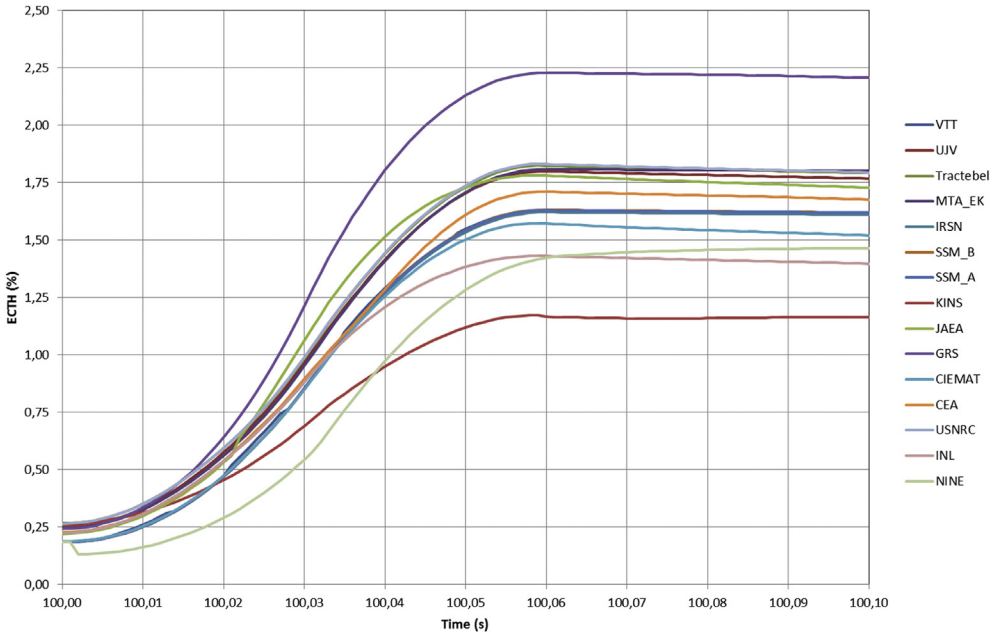

Fig. 4. ECTH reference calculations.

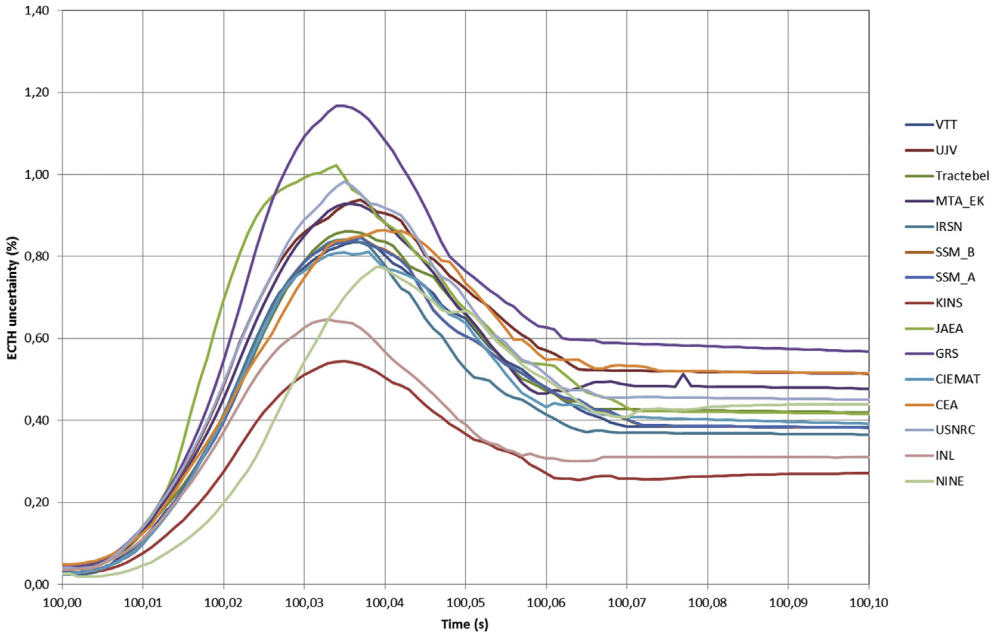

Fig. 5. ECTH uncertainty band widths.

- High coherence: this includes participants' results that are in strong agreement for uncertainty intervals and reference calculations. It corresponds to fuel thermal behavior outputs.
- Low coherence: this concerns participants' results with a conflict indicator equal to one but exhibiting coherent reference calculations and uncertainty intervals for a large majority of participants (i.e., the empty intersection is due to few participants that do not agree with the others). It is the case for fuel and clad mechanical behavior output except for SCH.
- No coherence: this concerns participants' results with a conflict indicator equal to one where the incoherence cannot be reduced by removing just a few contributions. It corresponds to thermal-hydraulic behavior output (TCO, boiling duration) and SCH. This strong lack of coherence can be explained by the combination of a large dispersion of reference calculations and narrow uncertainty bands, which is particularly noticeable for TCO and SCH.

4.3. Sensitivity analysis

Table 4 summarizes the sensitivity analysis performed. The injected energy and fuel enthalpy have been identified as

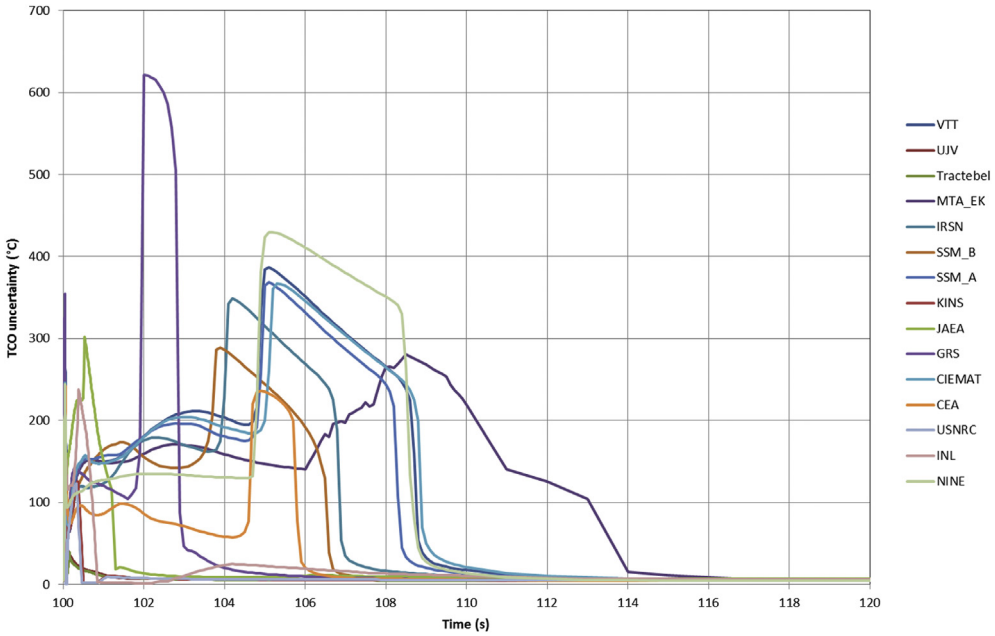

Fig. 6. TCO uncertainty band widths.

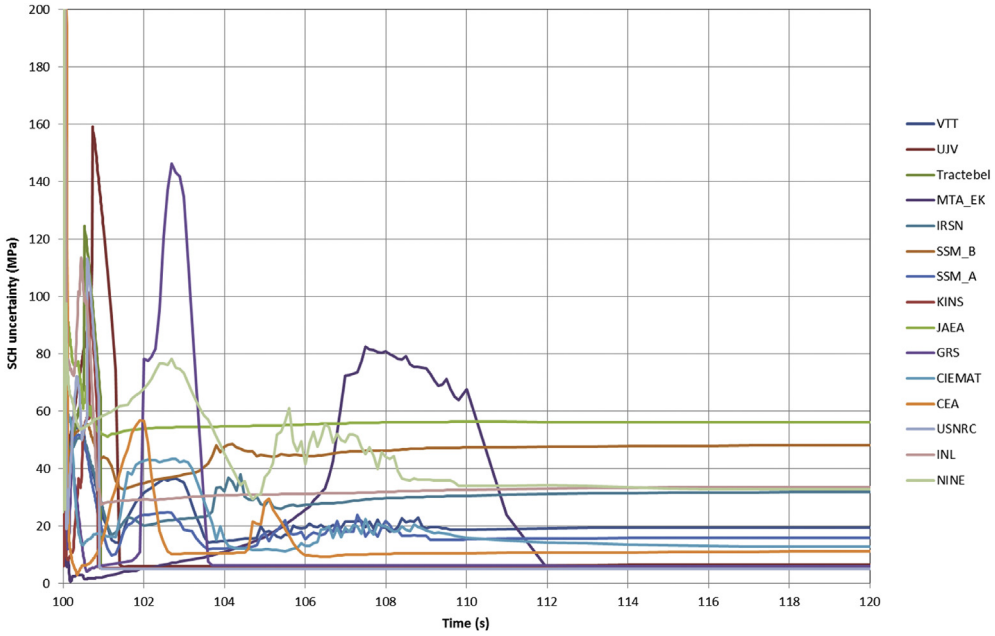

Fig. 7. SCH uncertainty band widths.

influential for all types of behaviors (fuel thermal, clad thermal, clad mechanical, and fuel mechanical behaviors) by a majority of participants. Input parameters related to the rod geometry (fuel and clad roughness and cladding inside diameter) as well as fuel thermal expansion model and FWHM are also found to be influential in this study.

On the contrary, several input parameters (clad thermal expansion and conductivity model, coolant velocity and pressure, filling gas pressure, fuel porosity and theoretical density, and cladding outside diameter) do not appear in Table 4 because they have been considered as influential by a very low percentage of participants.

One can also notice that there are more influential parameters for clad mechanical behavior than for the other types of behavior. This can be explained by the complex modeling of clad mechanical behavior, which depends on fuel pellet deformations and clad temperature.

It is also worth mentioning that some results associated with some input parameters are strongly affected by the utilized code. It is for example the case that clad-to-coolant heat transfer is influential for SCANAIR and not for FRAPTRAN. This can likely be attributed to differences in code versions. On the contrary, FWHM comes out as influential for FRAPTRAN, but not for SCANAIR.

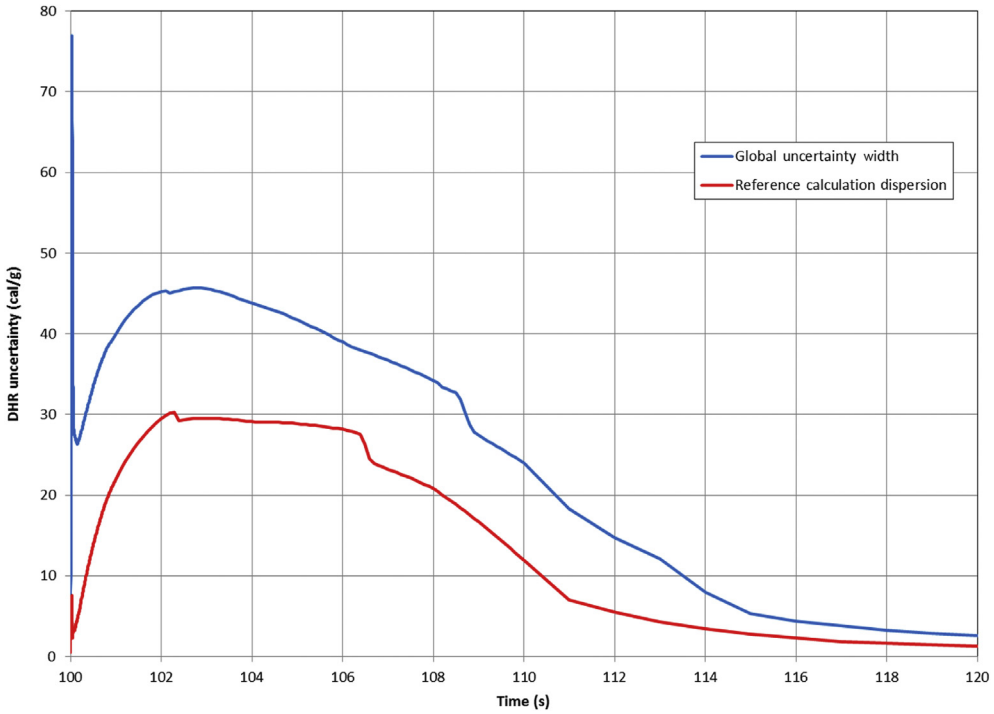

Fig. 8. DHR global uncertainty width and reference calculation dispersion.

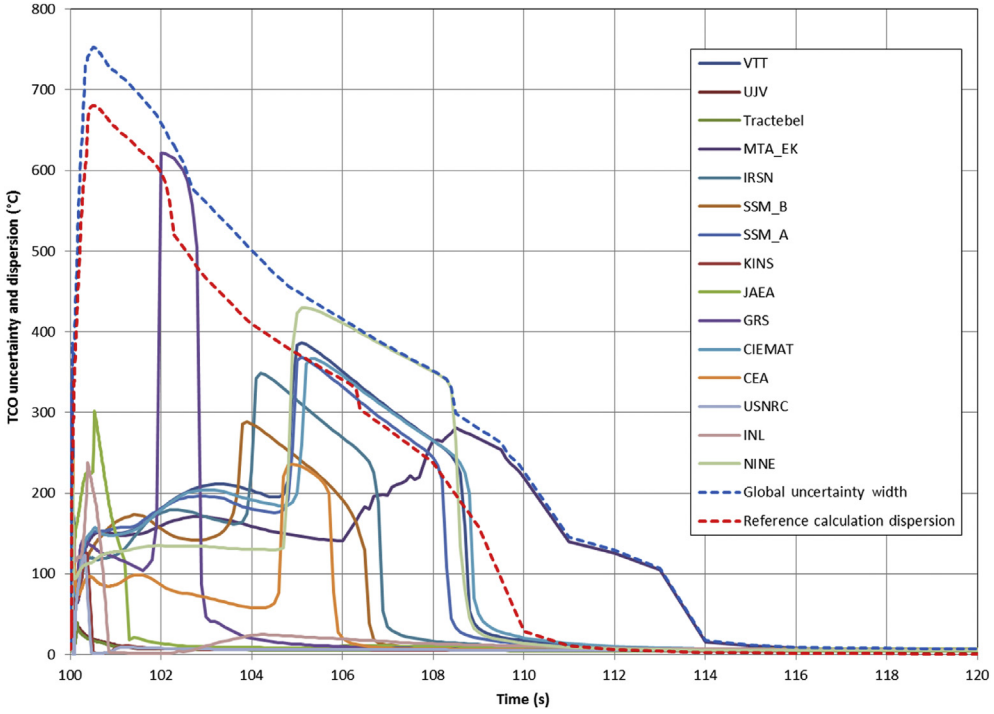

Fig. 9. TCO uncertainty bands for all contributors—TCO global uncertainty width and reference calculation dispersion.

5. Conclusion and recommendations

The results supplied by all participants were used in synthesis analyses performed according to the commonly agreed methodology. The uncertainty analysis has resulted in the following main observations:

- The pulse width uncertainty has a strong effect on the uncertainty results during the power pulse;
- The uncertainty band width is similar for all codes in the case of fuel thermal behavior outputs, and a high coherence is obtained for those parameters (participants' results are in strong agreement for uncertainty intervals and reference calculations);

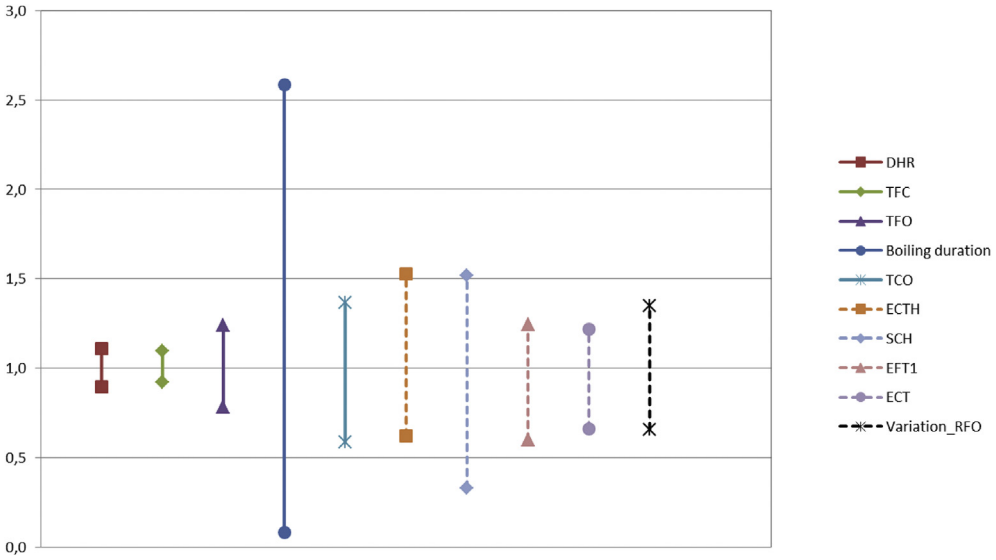

Fig. 10. Relative global uncertainty interval for the maximum value of each output parameter and boiling duration.

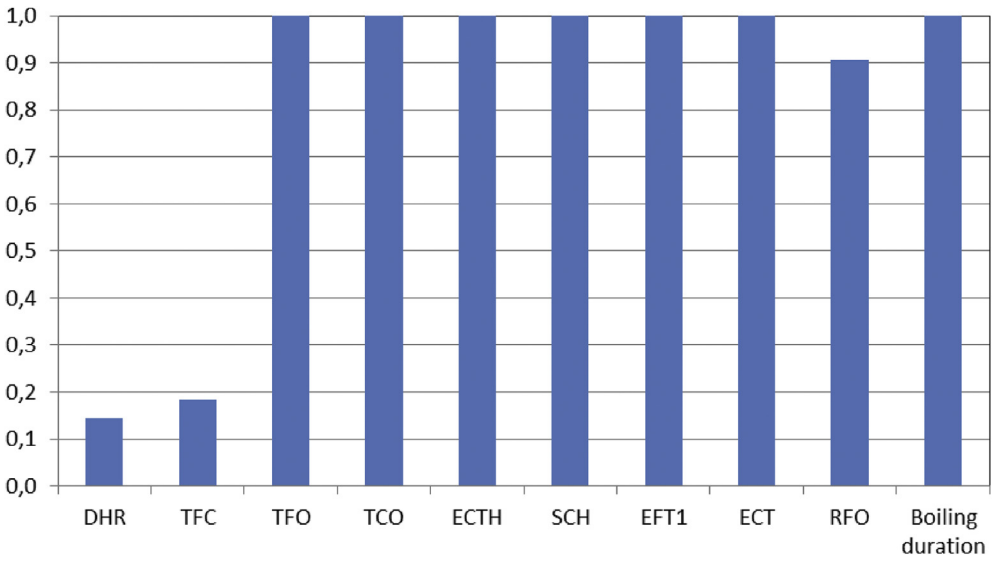

Fig. 11. Conflict indicator associated with each output (maximum values and boiling duration).

- Large uncertainty band width is observed for clad mechanical and thermal behavior outputs and fuel mechanical behavior outputs;
- A low coherence is observed for fuel and clad mechanical behavior outputs (except for stresses in the clad), but coherent reference calculations and uncertainty intervals are obtained for a large majority of participants;
- No coherence is observed for clad stress and thermal-hydraulic behavior outputs because of the combination of a large dispersion of reference calculations and narrow uncertainty bands for those parameters.

The sensitivity analyses for the maximum values of the main output parameters of interest have resulted in the following observations:

- The injected energy and fuel enthalpy have been identified as influential for all types of behaviors (clad and fuel thermal and mechanical behaviors) by a majority of participants;
- Input parameters related to the rod geometry (fuel and clad roughness and cladding inside diameter) as well as fuel thermal expansion model and FWHM were also identified as influential by this study;
- On the contrary, several input parameters (clad thermal expansion and conductivity model, coolant velocity and pressure, filling gas pressure, fuel porosity and theoretical density, and cladding outside diameter) have been considered as influential by a very low percentage of participants;
- There are more influential parameters for clad mechanical behavior than for the other types of behavior.

The second activity studies confirmed the conclusions from the first activity but also offered some new insights:

- Regarding fast transient thermal-hydraulic postdeparture from nucleate boiling behavior, there are major differences in the different modeling approaches resulting in significant

Table 4
Influential input parameters with respect to the type of behavior when focusing on maximum values.

	Fuel thermal (DHR, TFC)	Clad thermal (TCO)	Clad mechanical (ECTH, SCH)	Fuel mechanical (EFT1, RFO)
Cladding outside diameter				
Cladding inside diameter				
Fuel theoretical density				
Fuel porosity				
Cladding roughness				
Fuel roughness				
Filling gas pressure				
Coolant pressure				
Coolant inlet temperature				
Coolant velocity				
Injected energy in the rod				
Full mid height width				
Fuel thermal conductivity model				
Clad thermal conductivity model				
Fuel thermal expansion model				
Clad thermal expansion model				
Clad Yield stress				
Fuel enthalpy				
Clad to coolant heat transfer				

(A colored bar means that more than 50 % of the participants have identified the corresponding input parameter as influential for the type of behavior).

deviations between simulations. Unfortunately, there are currently no simple and representative experimental results that could allow us to validate (or not) the different approaches;
- The models of fuel and clad thermomechanical behavior and the associated materials properties should be improved and validated in RIA conditions;
- The different influential input parameters are identified for fresh fuel. For instance, injected energy, fuel enthalpy, parameters related to the rod geometry (fuel and clad roughness and cladding inside diameter), fuel thermal expansion model, and FWHM come out as influential regarding the maximum value of each output parameter of interest. However, the parameters with significant influence on the results for irradiated fuel could be different;
- Uncertainties cannot fully explain the scatter observed in the first activity results and during Phase I of this benchmark exercise;
- The specifics of used codes and user effects could play a more important role than uncertainties.

Based on the conclusions summed up above, the following recommendations can be made:

- To reduce user effect and code effect, the code development teams should as much as possible provide recommendations regarding the version of their codes to be used, the models and also the numerical parameters to be used (mesh size, time step, …);
- A complement of the RIA benchmark should be launched. This activity should be limited in time and should be focused on uncertainty and sensitivity analyses of an irradiated case, to identify the corresponding influential input parameters. In particular, uncertainties regarding fission gases distribution, fuel microstructure, clad corrosion state, and gap conductance should be investigated;
- This information (most influential input parameters for an irradiated case) will be useful in the perspective of a possible establishment of a phenomena identification and ranking table for RIA and could guide the future RIA tests and code improvements;
- Cooperation between existing experimental teams should be established in the area of clad-to-coolant heat transfer during very fast transients as well as in the area of the relevant fuel and clad thermomechanical modeling. The main objectives of this cooperation should be to collect and share all existing data and to formulate specific proposals to reduce the lack of knowledge and achieve common understanding of the subjects. This activity should address both out-of-pile and in-pile tests.

Finally, the conclusions of this work support the main recommendations proposed in the final report of first activity of the RIA fuel codes benchmark Phase II:

- Fuel and clad thermomechanical models (with the associated material properties) should be further improved and validated more extensively against a sound RIA database;
- Build-up of a comprehensive and robust database consisting of both separate-effect tests and integral tests should be pursued in the short term. In this way, both individual model validation and model integration into codes would be feasible. The database could be shared by the modelers, whenever possible, to ease the comparison of simulation results from various codes;
- The clad-to-coolant heat transfer in the case of water boiling during very fast transients is of particular interest, and capabilities related to modeling this phenomenon should be improved. To achieve this target regarding clad-to-coolant heat transfer, more separate-effect tests and experiments seem necessary;

- Models related to the evolution of the fuel-to-cladding gap should be improved and validated for RIA conditions as this has been shown to have a significant effect on fuel rod response. To reach this objective, in-reactor measurements of cladding strain during RIA simulation tests should be performed (or at least attempted).

Conflict of interest

There is no conflcit of interest.

Acknowledgments

The authors gratefully acknowledge the contributions of A. ARKOMA (VTT), F. BOLDT (GRS), A. DETHIOUX and T. DRIEU (Tractebel-ENGIE), H. BAN and C. FOLSOM (USU), V. GEORGENTHUM (IRSN), L.E. HERRANZ and I. SAGRADO GARCIA (CIEMAT), L.O. JERNKVIST (QT), H. JEONG (KINS), J. KLOUZAL (UJV), I. PANKA (EK), I. PORTER (USNRC), P.GOLDBRONN and J. SERCOMBE (CEA), Y. UDAGAWA (JAEA).

References

[1] NEA/CSNI/R, 1, Nuclear Fuel Behaviour Under Reactivity-Initiated Accidents (RIA) Conditions. State of the Art Report, Nuclear Energy Agency, OECD, Paris, France, 2010.

[2] NEA/CSNI/R, 7, Nuclear Fuel Behaviour Under Reactivity-Initiated Accidents (RIA) Conditions. Workshop Proceedings, Nuclear Energy Agency, OECD, Paris, France, 2010.

[3] NEA/CSNI/R, 7/VOL2, Reactivity Initiated Accident (RIA) Fuel Codes Benchmark, vol. 2, Nuclear Energy Agency, OECD, Paris, France, 2013.

[4] NEA/CSNI/R, 7/VOL1, Reactivity Initiated Accident (RIA) Fuel Codes Benchmark, vol. 1, Nuclear Energy Agency, OECD, Paris, France, 2013.

[5] NEA/CSNI/R, 6, Reactivity Initiated Accident (RIA) Fuel Codes Benchmark Phase II, vol. 1, Nuclear Energy Agency, OECD, Paris, France, 2016.

[6] NEA/CSNI/R, 6, Reactivity Initiated Accident (RIA) Fuel Codes Benchmark Phase II, vol. 2, Nuclear Energy Agency, OECD, Paris, France, 2016.

[7] NEA/CSNI/R, 1, Reactivity-Initiated Accident Fuel-Rod-Code Benchmark Phase II: Uncertainty and Sensitivity Analyses, Nuclear Energy Agency, OECD, Paris, France, 2017.

[8] H. Glaeser, GRS method for uncertainty and sensitivity evaluation of code results and applications, Sci. Technol. Nucl. Install. (2008), 798901.

[9] J. Zhang, J. Segurado, C. Schneidesch, Towards an industrial application of statistical uncertainty analysis methods to multi-physical modelling and safety analyses, in: Proc. OECD/CSNI Workshop on Best Estimate Methods and Uncertainty Evaluations, Barcelona, Spain, 16–18 November, 2011.

[10] E. Gentle, "Monte-Carlo Methods," Encyclopaedia of Statistics, 5, John Wiley and Sons, New-York, 1985, pp. 612–617.

[11] NEA/CSNI/R, 4, BEMUSE Phase VI Report – Status Report on the Area, Classification of the Methods, Conclusions and Recommendations, Nuclear Energy Agency, OECD, Paris, France, 2011.

[12] NEA/NSC, Benchmark for Uncertainty Analysis in Modelling (UAM) for Design, Operation and Safety Analysis of LWRs, in: Specification and Support Data for the Core Cases (Phase II), vol. II, Nuclear Energy Agency, OECD, Paris, France, 2014, Version 2.0.